Compact Mid-Infrared Trace Gas Sensor Based on Difference Frequency Mixing

Frank K.Tittel, David G. Lancaster, Dirk Richter
Rice Quantum Institute,Rice University, MS 366,Houston,TX 77005
(713)527-4833 (tel), fkt@rice.edu, http://www.ruf.rice.edu/~lasersci/

Lew Goldberg, Jeffrey P. Koplow
Optical Sciences Division, Naval Research Laboratories,Washington D.C. 20375-5672

ABSTRACT

The development of compact mid-IR sources using frequency-converted diode lasers has been demonstrated to be applicable for the ultra sensitive, selective, and real time detection of many trace gas species in the infrared spectroscopic fingerprint region, which contains virtually all the fundamental vibrational modes of molecules. This development of infrared laser sources has taken advantage of recent significant technological advances of semiconductor diode lasers and solid state lasers, new nonlinear optical materials, optical fiber and novel data acquisition techniques. Such sensors are able to detect molecules at the parts-per-billion (ppb) level in ambient air using infrared absorption spectroscopy either by monitoring trace gases in an open path or multi-pass cell configuration. Real world applications ranging from urban, industrial, rural emission studies to spacecraft habitat monitoring are described.

Keywords: Trace gas detection, Absorption spectroscopy, Diode lasers, Nonlinear optical frequency conversion

1. INTRODUCTION

Difference frequency mixing of near-infrared CW laser sources is a convenient technique to spectrally shift visible and infra-red lasers into the mid-infrared spectral region. By utilizing the recent commercial availability of novel nonlinear optical materials such as periodically poled lithium niobate (PPLN), and frequency-stable, single-mode diode lasers in the 0.8 to 1.5 μm spectral region, the key opto-electronic components exist to readily generate microwatt level radiation in the 3 to 5 μm range [1]. This spectral region is significant as many molecules have strong fundamental ro-vibrational absorption lines which permit sensitive and absolute concentration measurements. Our motivation is to develop a compact difference-frequency based trace gas sensor that is widely tunable, rugged and cost effective. The requirements for such a sensor include room temperature and real-time operation, narrow bandwidth to minimize spectral interference, adequate signal-to-noise for the available infrared detectors, a robust design (suitcase size), inherent frequency stability (with no mode hopping behavior) and wide wavelength tunability for multiple trace gas species detection.

In recent work, this group has reported trace gas sensors generating micro-watt level radiation based on difference-frequency mixing (DFM) (using discrete optical components positioned on a compact optical bench) of Fabry-Perot style diode lasers with a Nd: YAG laser [2] and a 1083 nm distributed Bragg reflector (DBR) diode laser [3]. The former system proved sufficiently robust to be used in a successful one-month field test involving high sensitivity H_2CO detection [4]. Widely tunable sensors based on difference frequency mixing of an extended cavity diode laser (ECDL) and a Nd: YAG laser have also been reported [5, 6], and are suitable for multicomponent trace gas monitoring. More recently a laboratory prototype DFM based gas sensor that utilizes single mode fiber delivery and rare earth doped fiber amplifiers producing up to 11 μW of tunable mid-infrared radiation was demonstrated [7-9]. The use of fiber delivery and fiber beam combining in these systems eliminates most of the routine alignment and stability problems inherent in difference frequency mixed sources using discrete optics. The work we report here is an optical sensor architecture that is widely tunable with virtually no re-alignment required and packaged for portable field operation. This sensor uses two frequency stable pump diode lasers, namely

Part of the SPIE Conference on Application of Tunable Diode and Other Infrared Sources for Atmospheric Studies and Industrial Processing Monitoring II • Denver, Colorado • July 1999
SPIE Vol. 3758 • 0277-786X/99/$10.00

an ECDL employing a high power, single frequency InGaAs laser and a 1083 nm distributed Bragg reflector (DBR) diode laser.

The recent development of such a field-ready fiber based DFG sensor with significantly improved conversion efficiency as compared to previous DFG architectures is reported in this work. In fact several trace gas species can be accessed in the 3.25 to 4.4 μm operating range of this DFG sensor. The predicted and experimentally measured PPLN phasematching conditions were also determined.

2.Experimental Configuration

The DFM based gas sensor as shown in Fig. 1 consists of a 25 mW ECDL which is continuously tunable from 814 to 870 nm (no mode hopping behavior is observed), and a 50 mW, 1083 nm distributed Bragg reflector diode laser (DBR). The output from the DBR diode laser is collimated using an aspheric lens, passes through a -45 dB optical-isolator, and is then coupled to a 6.6 μm core diameter single longitudinal mode (SLM) fiber terminated with a FC-APC style connector (threaded connector with the tip polished at 8° from normal incidence). A power of 12 mW of the seed radiation from the DBR diode laser is launched into the fiber. To increase the mechanical rigidity of the coupling arrangement, no beam correction optics were used and the entire diode/optics assembly was mounted on a compact stainless steel miniature-bench. Although higher coupling efficiencies into the fiber can be achieved, this was not necessary for this application, as only several mW of injected power at 1083 nm was required to saturate a Yb fiber amplifier. Fig. 2 depicts the Yb^{3+} doped double-cladding fiber amplifier characteristics. An amplifier output power of 590 mW at 1083 nm is obtained. This fiber was fusion spliced to the counter-propagating side (with respect to the 975-nm pump) of a 7.2 m ytterbium doped fiber amplifier pumped by a 975 nm, 2W-diode laser. A V-groove geometry was used to launch the amplifier pump light into the Yb^{3+} doped double-cladding fiber [9,10]. All amplifier components were packaged into a 9 x 11 x 2 cm^3 housing.

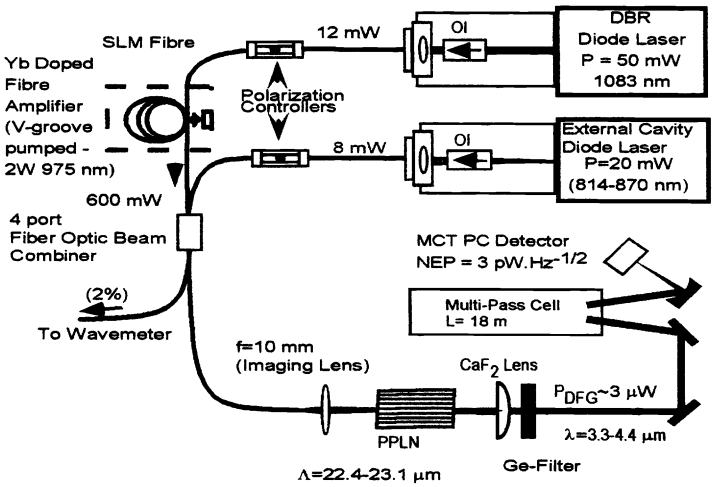

Fig. 1. Schematic diagram of the extended cavity diode laser and diode laser seeded 1083 nm Yb amplifier pumped difference frequency spectrometer.

The ECDL pump beam is passed through a –30 dB opto-isolator, and launched into a 5.5 μm core diameter SLM fiber using a single fiber-port assembly with a 48 % optical coupling efficiency. Coarse frequency tuning of a Littman type ECDL was achieved by 'rotation' of its tuning mirror with respect to the diffraction grating. The advantage of the Littman ECDL configuration is the consistent beam-pointing stability as a function of wavelength over the entire ECDL tuning range, ensuring consistent coupling into the optical fiber. Fine tuning and approximately linear repetitive scanning (at < 200 Hz) over single or multi-component absorption lines of up to ~25 GHz (0.83 cm^{-1}) was accomplished by linear current modulation of the DBR diode laser. Tuning the DBR diode laser was used in preference to the slower, non-

linear tuning available from the piezo-electrically-modulated grating of the ECDL that tended to reduce its spectral stability.

The pump wavelengths were combined by a four-port fiber coupler (2 in and 2 out), with losses of 9% and 8% at 1083 nm and 830 nm respectively. An additional advantage of the fiber coupler is the availability of several percent of power at each wavelength at the second output fiber, thereby allowing the use of an on-line fiber coupled wavemeter for frequency monitoring of the pump light. The linear polarization output from the launch fiber for a $e+e \rightarrow e$ difference frequency generation (DFG) process in the PPLN crystal was maintained by using two polarization controllers in the fiber delivery system. An achromat lens (f=10 mm; 0.25 NA) was used for imaging the fiber output (terminated with a FC-APC connector) into the PPLN crystal. A 19 mm long, 0.5 mm thick PPLN crystal with a broadband AR-coating applied to both end faces contained 8 quasi-phasematching channels (0.5 mm wide) from 22.4 - 23.1 μm in 0.1 μm increments. To characterize the PPLN crystal phasematching, the crystal was mounted on a temperature-controlled copper block (20 x 15 x 10 mm^3) heated by a resistive element that allowed the crystal to be operated at higher temperatures (< 250 °C). The temperature at the copper block surface was measured by a cold-junction compensated thermocouple (2 % accuracy). To reduce the thermal resistance between the copper block and crystal, thermal heat-sink compound was used. However, in the portable sensor configuration, the PPLN crystal was mounted on a single stage thermoelectric element, which could be operated at regulated temperatures ranging from 10 to 85°C. The lower temperature limit was set by concern for water condensation on the crystal faces.

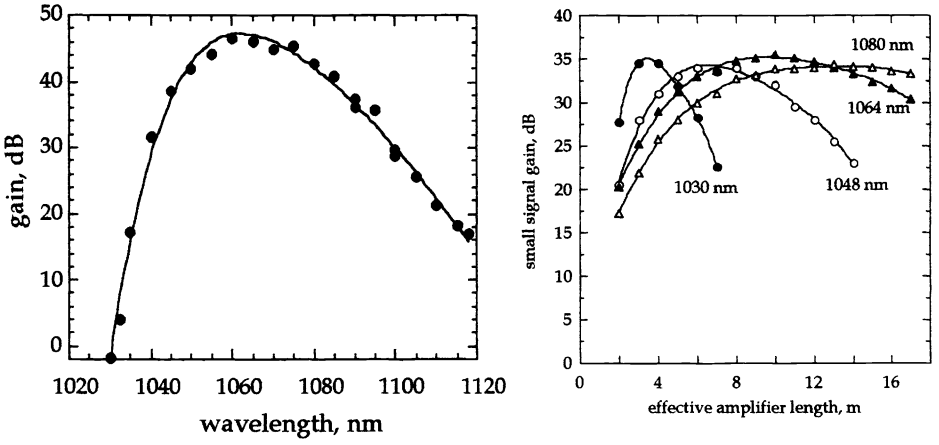

Fig. 2. Small signal gain of Yb-doped double cladding fiber amplifier vs wavelength (LHS) and effective amplifier length (RHS) for four injection seed wavelengths.

The DFG radiation was collimated by a 5 cm focal length CaF_2 lens and the residual pump light was blocked by a 3 mm thick AR-coated germanium filter. The radiation was either focussed directly on the three-stage Peltier cooled HgCdTe (MCT) detector for power measurements or directed through a 18 m pathlength multi-pass spectroscopic cell (physically 30 cm long) and then focussed onto the detector. In both cases the radiation was focussed onto the detector by use of a 5-cm focal length gold coated off-axis parabolic mirror. The MCT detector, with a 1 mm^2 active area and a measured noise equivalent power of 3 $pW/Hz^{-1/2}$, was DC coupled to a low-noise pre-amplifier operating in a photoconductive mode.

In order to reduce the size of the driver electronics required for the DBR diode laser, the Yb amplifier and the PPLN crystal Peltier element , compact OEM diode laser current and thermoelectric (TE) drivers were used. A TTL triggered relay controlled a beam shutter placed in front of the ECDL to allow a measurement of the detector dark voltage required for absolute transmission measurements. The data acquisition system used is similar to the one described in Ref. 4, and consisted of the output of the MCT detector pre-amplifier interfaced via a PCMCIA 16-bit A-D card to a notebook computer. Detector voltage was sampled at a rate of 100 kHz with a 9 kHz low pass filter (software implemented Gaussian filter). The data acquisition and analysis were controlled by Labview programming language.

The sensor including all electronics was placed on a 45 x 45 cm^2 optical breadboard, with an overall height of 12 cm. The weight was 25 kg and the entire sensor was then mounted in a reinforced

plastic suitcase for portability. Power was supplied by 4 x 5 V, 2 A linear power supplies, and 2 x ± 15 V, 200 mA linear power supplies. The ECDL used its commercial power supply and driver. Total power consumption is ~ 60 W.

To provide a continuous gas flow through the spectroscopic cell at a regulated pressure, a two-stage diaphragm pump was used in series with a pressure flow controller (MKS-640). A miniature Baratron pressure transducer (MKS-722) was used to measure the gas pressure just prior to the multi-pass cell. To reduce the interaction between the gas handling components and the gas mixtures, stainless steel or a teflon tubing was used throughout the gas delivery system. Furthermore, for measurement of reactive gases (such as H_2CO, HCl and NO_2) the gas handling system was maintained at ~ 40°C by use of heating tape. For the measurement of HCl which reacts strongly with water, and is in addition strongly polar, the gas system was purged for several hours by the use of high purity N_2 (H_2O concentration specified to be < 5 ppm)

2. Experimental Results

The mid-infrared DFG power as a function of wavelength is shown in Fig. 3. The right hand axis is the ECDL power (pump) available at the entrance facet of the PPLN. The 1083 nm power (signal) is kept constant at 540 mW. For incident powers of 6.2 mW and 540 mW of the pump and signal beams respectively, a maximum idler power of 2.8 μW at 3.46 μm was generated (corrected for losses of 3.4 % from the CaF_2 lens and a 4 % wavelength dependent loss of the Ge filter). The ECDL power delivered by the fiber peaks at 8.5 mW near 850 nm, corresponding to the gain center of the ECDL. The peak DFG conversion efficiency measured was 0.88 mW/W^2 for the 19 mm long crystal at 3.3 μm. In comparison, the theoretical DFG conversion efficiency yields 1.69 mW/W^2 [11]. Factors that contribute to the reduced experimental conversion efficiency include non-matching pump-beam mode field diameters in the fiber ($1/e^2$ diameters: 850 nm ~ 5.5 μm, 1083 nm ~ 6.6 μm) leading to incomplete overlap of the imaged pump beams in the crystal. The low NA (0.25) of the imaging lens will introduce spherical aberration into the focussed beam spots. Some non-uniformity in conversion efficiency across individual PPLN channels has also been observed.

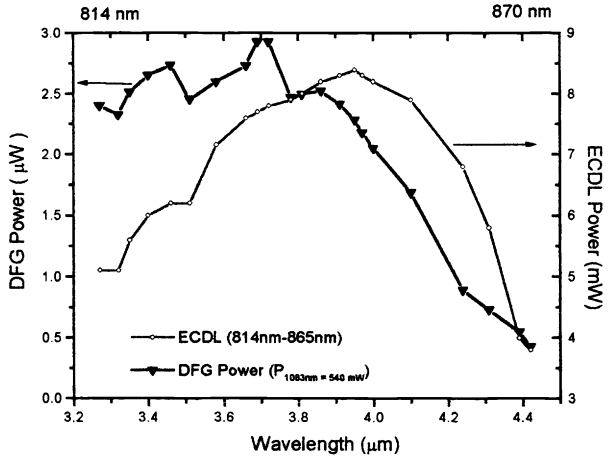

Fig. 3. DFG power as a function of idler wavelength and the ECDL power coupled into the optical fiber as a function of ECDL wavelength.

The measured PPLN phasematching and theoretically predicted phasematching are shown in Fig. 4 (using the Sellmeier coefficients published by Jundt [12]). For tuning the idler from 3.27 – 3.65 μm (Fig. 4)(LHS), the PPLN crystal was translated perpendicular to the optical axis across the 22.4 - 23.1 μm QPM channels (0.1 μm steps) at a constant temperature of 25 °C. DFG wavelengths of 3.65 to 4.4 μm were phasematched using the 23.1 μm QPM channel and crystal temperatures from 25 to 110°C (shown in fig. 4)(RHS). Agreement between theory and experiments is good, verifying that the Sellmeier coefficients for

PPLN are accurate out to at least 4.4 μm. This result indicates that any wavelength in the mid-infrared tuning range of the DFG gas sensor can be conveniently accessed using a combination of crystal temperature and grating period. If a PPLN crystal with grating periods of 22.4 – 23.3 μm in 0.1 μm steps is used, the entire tuning range of the sensor can be conveniently phasematched using different grating periods and temperatures from 11 to 43° C.

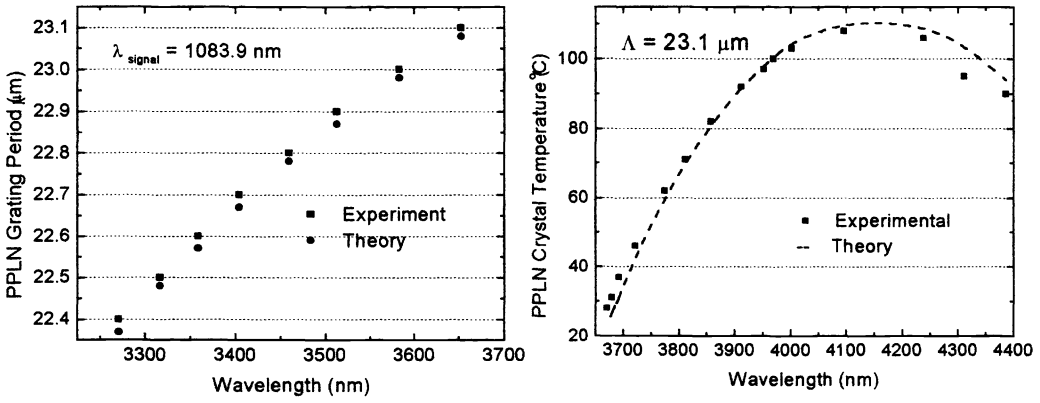

Fig. 4. Two quasi-phase matching approaches by changing nominal grating period (LHS) or temperature tuning at a fixed nominal grating period (RHS)

The linewidth of the DFG sensor was measured indirectly by acquisition of a low pressure Doppler broadened line spectrum. In Fig. 5 a portion of a Q-branch Doppler broadened (1 torr) CH_4 spectrum near 3.3 μm in a 3 cm length cell is shown. This spectrum was acquired at a sweep frequency of 70 Hz, and is an average of 20 scans. By fitting Gaussian absorption peaks to the individual absorption features, and then de-convolving the width with the calculated molecular Doppler width, 40 ± 5 MHz was determined for the DFG linewidth (assumed to be Gaussian). Although this linewidth is broader than expected (~ 10 MHz), it is significantly narrower than typical pressure broadened molecular linewidths, and provides high spectral selectivity.

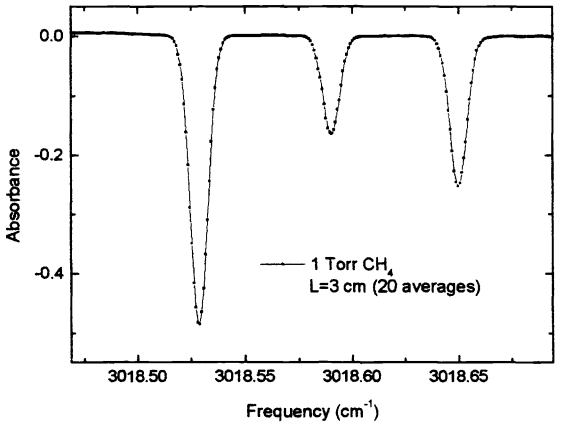

Fig. 5. Q-branch Doppler broadened 0.5 torr torr CH_4 spectrum near 3.3 μm. By fitting Gaussian absorption peaks to the individual absorption features and de-convolving the peak width with the calculated molecular Doppler width, an estimate of 195 ± 12 MHz was determined for the laser linewidth (assumed Gaussian).

Direct absorption spectra of 6 species of interest for trace gas detection that are within the 3.25 to 4.4 μm tuning range of the sensor including (a) CO_2, (b) N_2O, (c) H_2CO, (d) HCl, (e) NO_2 and (f) CH_4 have been acquired. These spectra have been obtained at reduced pressure (88 torr) in a multi-pass cell with an effective path length of 18 m using either calibrated gas mixtures or room air. The integrated line-shape area was used to determine the molecular concentrations. The peak-to-peak baseline noise evident from the recorded spectra is ± 0.02 %, and is due to etalon effects in the optical path of the modulated pump beam. To acquire individual spectra, the DFG based gas sensor was wavelength tuned by manually adjusting the ECDL wavelength (with reference to a wavemeter), and the phasematching conditions of the PPLN crystal were adjusted by a combination of translations to different QPM periods and temperature changes. No additional re-alignment of the sensor was required when the wavelength was changed indicating that complete automation of sensor tuning should be straightforward using say a stepper motor. To remove baseline irregularities caused by etalons in the beam paths, a 3rd order polynomial was simultaneously fitted with a pressure broadened Lorentzian lineshape using a non-linear least squares algorithm (Levenberg-Marquardt). The data processing and fitting was accomplished in near real-time (<2s). For each spectrum the signal was averaged over the specified time, and subsequently the detector dark voltage was measured (50 averages) to allow calculation of the absolute absorption.

In Table 1 the data acquisition parameters are listed, and the measured spectral characteristics and concentrations are compared to the spectral data predicted from the Hitran96 database and the calibrated concentrations of the measured trace gases. In the case of HCl, the concentration was obtained from a calibrated cylinder specified at 24.4 ppm (in N_2) which we measured the HCl concentration to be 19.5 ± 0.2 ppm. This measurement used alternatively the $H^{35}Cl$ line at 2944.913 cm^{-1} and the $H^{37}Cl$ line at 2942.721 cm^{-1} (S = 5.033 x 10^{-19} cm/ molecule and 1.606 x 10^{-19} cm/ molecule, respectively). The minimum detectable concentration (MDC) value stated in Table 1 was calculated for a single measurement, and assumes a S/N = 1, and an absorption measurement sensitivity of 4 x 10^{-4}.

Gas species	Scan range (cm^{-1})	Averaging time (sec)	Pressure (torr)	Scan Center cm^{-1}, (μm)	Meas. Conc.	Specified Concentration	MDC (L=18m)
CO_2	0.34	2.1	88	2387.2 (4.19)	444 ppm	Room air	460 ppb
N_2O	0.29	2.1	88	2572.1 (3.89)	315 ppb	Room air	95 ppb
H_2CO	0.27	2.1	88	2831.7 (3.53)	860 ppb	862 ± 15 ppb	54 ppb
HCl	0.33	2.1	87	2843.6 (3.52)	19.5 ppm	24.4 ppm (± 5%)	9 ppb
NO_2	0.28	2.1	88	2881.8 (3.47)	7634 ppb	13.0 ppm (± 5%)	259 ppb
CH_4	0.32	2.1	88	3028.7 (3.30)	1756 ppb	Room air	23 ppb

Table 1. Data acquisition parameters, measured spectral characteristics and concentrations compared to the spectral data predicted by the Hitran96 database and the calibrated concentrations of 6 measured trace gas species.

The overall instrument performance, including repeatable precision and suitability of the sensor for long term measurements was assessed by monitoring of a discrete CH_4 line at 3038.751 cm^{-1} for an extended period of time. In this experiment a calibrated 1772.7 ± 1 ppb mixture of CH_4 in air [13] was continuously passed through the multi-pass cell at a pressure of 88 torr. The experimental results are shown in Fig. 6. Over a 19 minute period (131 measurements, 4s average per measurement), the gas sensor measured a concentration of 1830 ppb, which is within 3.1 % of the calibrated concentration. If the ±2 %

uncertainty in the path length of the multipass gas cell is taking into account the agreement is closer. This CH_4 concentration measurement used the Hitran96 predicted linestrength of 9.519×10^{-20} cm/molecule for the 3028.751 cm^{-1} line. The measurement standard deviation was $\pm$ 0.8 % ($\pm$ 15 ppb) which corresponds to an absorption sensitivity of $\pm 2 \times 10^{-4}$.

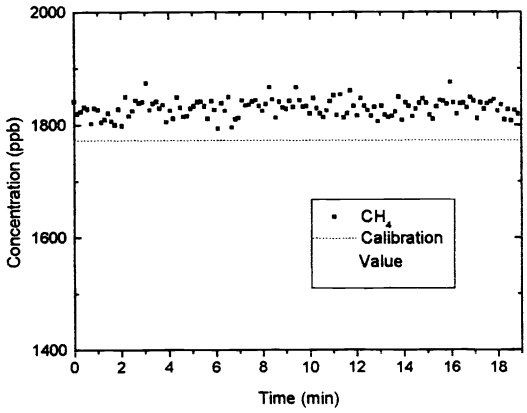

Fig. 6. Measured CH_4 concentration for a 19 minute period using a continuously flowing gas mixture at 88 torr. A spectrum was acquired every 8.7 s and was averaged for 4 s. We measured a concentration of 1829.5 $\pm$ 15.4 ppb which compares favorably with the calibrated CH_4 concentration of 1773 ppb [13].

3. Discussion and Conclusion

The use of fiber delivery and a WDM for beam combination has significantly improved the robustness and wavelength tuning capability of the sensor. During routine operation, the DFG power level was found to be stable over multi-day operation. To ensure stable sensor operation, care needed to be taken in packaging of the optical fibers, as any movement or pressure on the optical fibers effects the polarization of the pump beams and hence decreases the DFG conversion efficiency. Furthermore, the alignment was maintained (indicated by a constant DFG power level) when the sensor was relocated to an outside environment. These results are in contrast to our experience with the operation of DFG sensors based on discrete optics that required periodic minor re-alignments because of mirror and lens mount relaxation [3,4]. In addition by utilizing an efficient high-power Yb doped fiber amplifier we have eliminated the need for a high-power narrow linewidth source. This has been replaced with the requirement for a low-power (~ several mW) amplifier seed source which can operate anywhere within the broad gain bandwidth of the Yb fiber amplifier (1020 – 1120 nm).

We have acquired spectra of 6 common trace gas species to demonstrate the versatility of this diode laser based DFG sensor. The specific spectral lines we used for the detection of each molecule were chosen on the basis of the expected concentrations present and known interfering species. However because of the extended continuous tuning range of this sensor, alternate absorption lines could be chosen for detection of low/high gas concentrations or in the presence of interfering molecule absorptions.

From this work, it was deduced that the current detection sensitivity is limited by the occurrence of etalons in the baseline, presently corresponding to absorbances of $\pm 2 \times 10^{-4}$. To compensate for these etalons and increase the absolute sensitivity of the absorption measurement, the use of a balanced detection scheme [14] is expected to increase the routine detection limit to ~ 5×10^{-5}. This will involve a wedged

beam sampling mirror placed prior to the multi-pass cell which directs a small amount of the beam to a second detector, thereby allowing the non-linear baseline to be normalized using the sampled baseline. This technique will not remove the fringes that originate from the multiple mirror reflections in the multi-pass cell, but it is possible to use a digital notch filter to reduce these etalon fringes. For extended operation the frequency drift of the diode lasers must be controlled, this is particularly pronounced until the sensor suitcase reaches a steady state temperature. Such active temperature control of the DBR diode laser requires a frequency reference based on an appropriate spectral feature acquired from a reference gas cell (which is periodically inserted into the beam path). Furthermore, a PPLN crystal with a 'fan-out' QPM grating design [15] will replace the discrete channel PPLN crystal which will permit continuous DFG scans to be conducted by synchronously tuning one of the pump wavelengths while translating the crystal. DFG power scaling using watt level in-line fiber amplifiers [16] is expected to increase the available mid-IR DFG power by factors of 10 to 100, thereby improve the detector signal-to-noise, or allow the use of IR detectors operating at room temperature without the need of Peltier cooling.

In conclusion, we have demonstrated a narrow bandwidth DFG sensor with a 3.25 – 4.30 μm tuning range and generating up to 3 μW in the spectroscopically important 3-5 μm 'fingerprint' region. By fiber coupling the pump sources and using a fiber coupler for combining the pump beams, routine alignment tasks have been eliminated. We have demonstrated sensitive, selective, and real-time detection of CH_4 at 3.3 μm by monitoring a calibrated mixture of CH_4 (1773 ppb) over a 20 minute period and measuring a concentration of 1829.5 ppb with standard deviation of ± 0.8 %. The measured standard deviation error corresponds to an absorption sensitivity of $\pm 2 \times 10^{-4}$. Furthermore, we have demonstrated the versatility of this sensor by recording spectra of six trace gas species: CO_2 (4.19 μm), N_2O (3.89 μm), H_2CO (3.53 μm), HCl (3.52 μm), NO_2 (3.47 μm) and CH_4 (3.30 μm). It will be possible to use the same device architecture in the future to extend the current spectral regime to longer wavelengths (5-16 μm) by using quasi-phasematched GaAs when this material becomes available [17, 18].

ACKNOWLEDGEMENTS

Financial support was provided by the National Aeronautics and Space Administration (NASA), the Texas Advanced Technologies Program, the National Science Foundation, and the Welch Foundation.

REFERENCES

1. K. P. Petrov, L. Goldberg, W.K. Burns, R.F. Curl, F.K. Tittel, "Detection of CO in air using diode-pumped 4.6 μm difference frequency generation in quasi-phase-matched $LiNbO_3$," *Opt. Lett*, 21, 86-88 (1996)
2. T. Töpfer, K.P. Petrov, Y. Mine, D. Jundt, R.F. Curl, F.K. Tittel, "Room temperature mid-infrared laser sensor for trace gas detection," *Appl. Opt.* 36, 8042-8049 (1997)
3. D. Richter, D. G. Lancaster, R. F. Curl, W.Neu, F.K. Tittel, "Compact mid-infrared trace gas sensor based on difference-frequency generation of two diode lasers in periodically poled $LiNbO_3$," *Appl. Phys. B* 67, 347-350 (1998)
4. D. G. Lancaster, D. Richter, R. F. Curl and F. K. Tittel, "Real-time measurements of trace gases using a compact difference frequency based sensor operating at 3.5 μm," *Appl. Phys. B* 67, 339-345 (1998)
5. K.P. Petrov, R.F. Curl, F.K. Tittel, "Compact laser difference-frequency spectrometer for multi-component trace gas detection," *Appl. Phys. B* 66, 531-538 (1998)
6. M. Seiter, D. Keller, M.W. Sigrist, "Broadly tunable difference-frequency spectrometer for trace gas detection with noncollinear critical phase-matching in $LiNbO_3$," *Appl. Phys. B* 67, 351-356 (1998)
7. L. Goldberg, J. Koplow, D.G. Lancaster, R. F. Curl, F.K. Tittel,"Mid-IR difference frequency generation source pumped by a 1.1 μm – 1.5 μm dual-wavelength fiber amplifier for trace-gas detection," *Opt. Lett.* 23, 1517-1519 (1998)
8. D.G. Lancaster, L. Goldberg, J. Koplow, R.F. Curl, F.K. Tittel, "Fiber coupled difference frequency generation in periodically poled $LiNbO_3$," *Elect. Lett.*, 34, 13, 1345-1346 (1998)
9. L. Goldberg, J.P. Coplow, R.P. Moeller, D.A.V. Kliner, "High-power superfluorescent source with a side-pumped Yb-doped double-cladding fiber," *Opt. Lett.*, 23, 1037-1039 (1998)
10. L. Goldberg, B. Cole, E. Snitzer, *Electron. Lett.* 33, 2127-2129 (1997)

11. P. Canarelli, Z. Benko, R.F. Curl, F.K. Tittel, "Measurement of nonlinear coefficient and phase matching characteristics of $AgGaS_2$," *J. Opt. Soc. Amer. B*, 9, 197-202 (1992)
12. D.H. Jundt, *Opt. Lett.* 22, 1553-1555 (1997)
13. Courtesy of E. Dlugokencky, NOAA, Climate Monitoring & Diagnostic Laboratory, Boulder CO
14. M. G. Allen, K. L. Carleton, S.J. Davis, W. J. Kessler, C.E. Otis, D.A. Palombo, D.M. Sonnenfroh, *Appl. Opt.* 34, 3240-3249 (1995)
15. P. E. Powers, T. J. Kulp, S. E. Bisson, *Opt. Lett.* 23, 159, (1998)
16. L. Goldberg, J. Koplow, D.A.V. Kliner, *Opt. Lett.*, 24, 673, (1999)
17. D. Zheng, L. A. Gordon, Y.S. Wu, R.S. Feigelson, M.M. Fejer, R.L. Byer, K.L. Vodopyanov, "16-μm infrared generation by difference-frequency mixing in diffusion-bonded-stacked GaAs," *Opt. Lett.* 23, 1010-1012, (1998)
18. L. A. Eyres, C. B. Ebert, J. S. Harris Jr, M. M. Fejer, *CNOM Annual Report 1997-1998*, Stanford University